Anesthesiology
1998; 88:461-72

Fructose-1,6-Bisphosphate Preserves Adenosine Triphosphate but Not Intracellular pH during Hypoxia in Respiring Neonatal Rat Brain Slices

Maryceline T. Espanol, Ph.D.,* Lawrence Litt, Ph.D., M.D.,† Koh Hasegawa, M.D., Ph.D.,‡ Lee-Hong Chang, Ph.D.,§ Jeffrey M. Macdonald, Ph.D.,* George Gregory, M.D.,‖ Thomas L. James, Ph.D.,# Pak H. Chan, Ph.D.**

Background: **Fructose-1,6-bisphosphate (FBP) sometimes provides substantial cerebral protection during hypoxia or ischemia. $^{31}P/^{1}H$ nuclear magnetic resonance spectroscopy of cerebrocortical slices was used to study the effects of FBP on hypoxia-induced metabolic changes. In addition, ^{13}C-labeled glucose was administered and ^{13}C nuclear magnetic resonance spectroscopy was used to search for FBP-induced modulations in glycolysis and the pentose–phosphate pathway.**

Methods: **In each experiment, 80 slices (350 μm) obtained from ten 7-day-old Sprague-Dawley rat litter mates were placed together in a 20-mm nuclear magnetic resonance tube, perfused, and subjected to 30 min of hypoxia ($P_{O_2} < 3$ mmHg). Nine experiments were performed, with n = 3 in each of three groups: (1) no treatment with FBP; (2) 60 min of prehypoxia treatment with FBP (2 mM); and (3) 60 min of posthypoxia treatment with FBP (2 mM). $^{31}P/^{1}H$ Interleaved nuclear magnetic resonance spectra at 4.7 T provided average adenosine triphosphate, intracellular *p*H, and lactate. Cresyl violet stains of random slices taken at predetermined time points were studied histologically. Some experiments had [2-^{13}C]glucose in the perfusate. Slices from these studies were frozen for perchloric acid extraction of intracellular metabolites and studied with high-resolution ^{13}C nuclear magnetic resonance spectroscopy at 11.75 T.**

Results: **With no pretreatment with FBP, hypoxia caused an ≈50% loss of adenosine triphosphate, an ≈700% increase in lactate, and a decrease in intracellular *p*H to ≈6.4. Pretreatment with FBP resulted in no detectable loss of adenosine triphosphate, no increase in lactate, and minimal morphologic changes but did not alter decreases in intracellular *p*H. ^{13}C Nuclear magnetic resonance spectra of extracted metabolites showed that pretreatment caused accumulation of [1-^{13}C]fructose-6-phosphate, an early pentose–phosphate pathway metabolite. Posthypoxic treatment with FBP had no effects compared with no treatment.**

Conclusions: **During severe hypoxia, pretreatment with FBP completely preserves adenosine triphosphate and almost completely preserves cell morphology but does not alter hypoxia-induced decreases in intracellular *p*H. Pretreatment also substantially augments the flux of glucose into the pentose–phosphate pathway. (Key words: Brain slice; metabolism; nuclear magnetic resonance; spectroscopy.)**

PREVIOUS *in vivo* and *in vitro* animal studies found that pretreatment with fructose-1,6-bisphosphate (FBP) provides protection of hemodynamic and vital organs during shock, hypoxia, and ischemia.[1-5] Subsequent studies that focused on cerebral hypoxia and ischemia found that pretreatment with FBP reduced central nervous system injury.[4-9] When FBP is cerebroprotective during oxygen deprivation, adenosine triphosphate (ATP) is preserved and levels of extracellular glutamate are reduced.[10] Such findings have inspired hope that FBP ultimately might serve a role or provide valuable mechanistic insight in the prophylaxis and therapy for human cerebral ischemia. Certain other studies, however, found that FBP fails to provide protection during cerebral ischemia.[11-13] More significantly, there is no

* Postdoctoral Research Associate, Department of Pharmaceutical Chemistry.

† Professor, Departments of Anesthesia and Radiology; Associate, Cardiovascular Research Institute.

‡ Visiting Research Associate, Department of Anesthesia.

§ Adjunct Assistant Professor, Department of Pharmaceutical Chemistry.

‖ Professor, Departments of Anesthesia and Pediatrics; Associate, Cardiovascular Research Institute.

Professor and Chairman, Department of Pharmaceutical Chemistry.

** Professor, Departments of Neurosurgery and Neurology.

Received from the Departments of Anesthesia, Pharmaceutical Chemistry, Neurology, Neurosurgery, Radiology, and the Cardiovascular Research Institute, The University of California, San Francisco, San Francisco, California. Submitted for publication May 14, 1997. Accepted for publication October 16, 1997. Supported in part by National Institutes of Health research grants GM34767 (to Dr. Litt), NS14543 (to Dr. Chan), NS25372 (to Dr. Chan), RR03841 (to Dr. James), and NS93001 (to Dr. Gregory); and the Whitaker Foundation and the American Heart Association (Dr. Chan).

Address reprint requests to Dr. Litt: Department of Anesthesia, University of California, San Francisco, Box 0648, 521 Parnassus Avenue, San Francisco, California 94143-0648. Address electronic mail to: llitt@itsa.ucsf.edu

comprehensive explanation of the mechanisms by which FBP provides protection. Some have suggested an empirical conclusion—that there is lack of central nervous system protection if: (1) FBP is given *after* ischemia, or (2) ischemia is "too severe," or (3) the administered FBP dose is lower than a threshold value, typically 500 mg/kg.[4,11-13] We note two exceptions regarding pretreatment. Kuluz *et al.*[8] found that postischemic administration of FBP reduced infarct size in a rat middle cerebral occlusion model, and Sola *et al.*[5] demonstrated that it reduced central nervous system injury in neonatal rats after hypoxia. In both studies, there was a threshold for central nervous system protection.

Because we thought that noninvasive nuclear magnetic resonance (NMR) spectroscopy of respiring brain slices might demonstrate fundamental metabolic differences when FBP is protective, we used noninvasive $^{31}P/^{1}H$ NMR spectroscopy to study the effects of pretreatment with FBP on hypoxia-induced changes in intracellular ATP, intracellular *p*H (pH_i), and lactate. It has been postulated that FBP might sustain levels of ATP by entering cells and acting as a metabolic substrate that normally requires ATP expenditures. In glycolysis, two ATP molecules are expended in converting glucose to FBP: one by hexokinase, which phosphorylates glucose on cell entry, and another by phosphofructokinase, which phosphorylates fructose-6-phosphate (F6P). Intracellular entry of FBP would spare these ATP costs. FBP might also stimulate the pentose-phosphate pathway (PPP; also called the phosphogluconate pathway), which is known to be present in nerve endings, where it is activated during stresses that require local repair or reduction of oxidative toxins.[14] We therefore also explored the feasibility of using ^{13}C NMR spectroscopy to detect FBP-induced modulations of glycolytic and PPP metabolites after administering ^{13}C-labeled glucose. We also performed histologic examinations of 20-μm thick Nissl-stained sections cut from slices that had been removed at predetermined times in the protocol.

Materials and Methods

Experimental Design

Obtaining slices of high metabolic integrity requires minimizing injury from two sources: postdecapitation ischemia and mechanical trauma during brain removal and slice cutting. To combat the former, we used isoflurane/oxygen anesthesia and mild hypothermia before decapitation.[15-18] To combat the latter we worked quickly, taking only 30 sec from decapitation to placement of four slices in oxygenated medium, and we used a technique established earlier in which only brain surface slices are obtained,[19] thereby assuring that only one side of each slice was traumatized during cutting. Electrophysiologists who use brain slice preparations for microelectrode investigations of single synapses have long known that slice neurons are edematous, metabolically impaired, and electrically dysfunctional in the immediate postdecapitation period but that after 2 h of optimum care, morphology, metabolism, and synaptic function return to normal.[20-22] We also have shown that our $^{31}P/^{1}H$ NMR spectra from brain slices are identical to *in vivo* NMR spectra, except for increases in amplitude of the inorganic phosphate (P_i) and lactate peaks.[15-18] The increases in P_i and lactate are consistent with the notion of an $\approx$50-μ-thick injury layer at the cut surface.[20] We recently confirmed this estimate for the size of the injury layer in c-fos and heat shock protein 70 *in situ* hybridization studies of slices, in which the size and state of the injury layer was made quantifiable by immunohistochemical stains sensitive to apoptosis and deoxyribonucleic acid damage.[23] Messenger ribonucleic acid for c-fos and heat shock protein 70, are, respectively, markers of neuronal insult (intracellular calcium excess) and injury (intracellular protein denaturation). The $\approx$50-μ region that we identified as the mechanically traumatized injury layer was further confirmed as such by showing that decreases in postdecapitation neuronal damage occurred only in that region as a response to immediate postdecapitation treatment with dizocilpine (MK-801). (Neurons in cell culture previously were shown to be protected by dizocilpine from mechanical trauma, *i.e.*, from mechanical streaking of the culture plate.[24]) We also have observed that perfused slices undergo mild edema immediately after decapitation, that histologic morphology returns to normal within 2 h,[17] and that messenger ribonucleic acid expression of heat shock protein 70 does not occur in slices if hypoxia is avoided.[23]

Our protocol for obtaining cerebrocortical slices (350 μ thick) was approved by the Committee on Animal Research at University of California, San Francisco. Details of animal protocols, $^{31}P/^{1}H$ NMR experimental protocols, and artificial cerebrospinal fluid composition its perfusion system have been described previously.[15-18] In each experiment, 80 live cerebrocortical slices (350-

μm thick and ≈3.2 g total wet weight) were obtained from 20 7-day-old Sprague-Dawley rats and perfused in a glass NMR tube 20 mm in diameter. Interleaved $^{31}P/^{1}H$ NMR spectroscopy studies were performed at 4.7 T. Experiments began 120 min after metabolic recovery (defined as the return of the phosphocreatine:ATP ratio to ≈1.5 after decapitation ischemia.[15-18] Five-minute NMR acquisitions resulted in spectra from which we determined ATP, phosphocreatine, pH_i and extracellular pH (pH_o), and the ratio of intracellular lactate to *N*-acetyl-aspartate (NAA). In this system, NAA levels in *ex vivo* ^{1}H NMR spectra remain constant for ≈4 h if the slices are killed and perfusion is continued. In previous studies,[17] we demonstrated that our slices are robust and that $^{31}P/^{1}H$ NMR spectra each remain constant for >16 h if hypoxia is not induced, *i.e.,* if slices are perfused only with oxygenated media.

Nine $^{31}P/^{1}H$ NMR spectroscopy studies of hypoxic slice ensembles were performed. There were three complete studies (n = 3 in each of three groups): (1) no treatment, (2) pretreatment with FBP, and (3) posttreatment with FBP. The FBP concentration, 2 mM, was selected from earlier *in vitro* studies that found FBP to be protective.[4-6,9] FBP was obtained as D-fructose-1,6-bisphosphate trisodium salt octahydrate (≈99% pure; Fluka Chemical Corporation, Ronkonkoma, NY). Artificial cerebrospinal fluid osmolarity, measured with a Wescor vapor pressure osmometer (Logan, UT), was not significantly changed by the addition of 2 mM FBP (304.8 ± 2.8 *vs.* 308.2 ± 1.6 milliosmoles per liter [mOsM], for artificial cerebrospinal fluid alone *vs.* artificial cerebrospinal fluid + 2 mM FBP). For the FBP pretreatment group, slices were initially perfused for 60 min with oxygenated, artificial cerebrospinal fluid containing 2 mM FBP. For the no treatment group, no FBP was administered before or after hypoxia. After the 60-min perfusion, 30 min of hypoxia was induced in two steps: (1) 10-min perfusion of artificial cerebrospinal fluid that was made hypoxic via equilibration with 5% CO_2/95% N_2 (with or without 2 mM FBP); and (2) subsequently cessation of perfusate flow for 20 min. The total hypoxic episode was 30 min in each case. Artificial cerebrospinal fluid P_{O_2} was always <3 mmHg, as measured with a polarographic oxygen electrode (Cole-Parmer Model 9071 DO_2 meter equipped with a "Clark"-type polarographic oxygen electrode, UK). During the 30-min hypoxia episode, a flow of 100% N_2 was maintained in the gas region of the tissue perfusion chamber (above the fluid). After hypoxia, a 60-min recovery period was accomplished by perfusing the slices with artificial cerebrospinal fluid that had been equilibrated with 95% O_2/5% CO_2. This artificial cerebrospinal contained no FBP, corresponding to the no treatment and FBP pretreatment groups, whereas the post-hypoxic artificial cerebrospinal fluid contained 2 mM FBP, corresponding to the FBP posttreatment group. Slices were removed for fixation at five different predetermined times in the protocol for sectioning, cresyl violet staining, and histologic examinations. Removal times corresponded to postdecapitation, end of decapitation recovery (or beginning of NMR studies), beginning of hypoxia, end of hypoxia, and end of recovery.

Six high-resolution ^{13}C NMR spectroscopy studies of metabolite extracts were performed at 11.75 T in two separate series of hypoxia experiments; n = 3 in each of the two groups (with and without pretreatment with FBP). In each group, 5 mM [2-^{13}C]glucose (Cambridge Isotope Laboratories, Andover, MA) was administered during the 60 min before hypoxia; otherwise, the protocol was exactly the same as in $^{31}P/^{1}H$ *ex vivo* NMR studies. The metabolite extraction procedure is described in the section on ^{13}C NMR methods.

Histology

Slices taken from the perfusion chamber at different predetermined times were transferred to tubes containing 10% formalin in phosphate-buffered 0.9% saline solution (pH ≈7). After 24-72 h, the tissues were washed, dehydrated, and embedded in paraffin. Adjacent 10-μm-thick sections were cut in the plane of the slices, stained with cresyl violet (Nissl stain), and examined with phase contrast light microscopy (Zeiss Axioskop Model 20, Thornwood, NY). Representative fields of 50-140 adjacent cells, corresponding to areas of ≈10^4 μm^2, were photographed after counting shrunken and dead neurons.

Determination of Free, Ionized Ca^{2+} in the Perfusate

Because of the possibility that FBP might chelate calcium, nine sets of six measurements were made of free Ca^{2+} in separate experiments. Each measurement was from a 100-μl aliquot of medium withdrawn from the bottom of the NMR tube (slice chamber). The nine sets were for three different experimental conditions: n = 3 for FBP-treated slices; n = 3 for untreated slices; and n = 3 for perfusate alone (no slices). The six measurements in each set corresponded to different sampling

times: (1) before perfusion with 2 mM FBP; (2) after 30 min of pretreatment with 2 mM FBP (*i.e.,* after half of the pretreatment); (3) after 60 min of pretreatment with 2 mM FBP (*i.e.,* end of pretreatment); (4) after 30 min of hypoxia; (5) after 60 min of reperfusion recovery; and (6) after 120 min of reperfusion recovery. Recordings were obtained using a Ca^{2+}-selective ion electrode (Orion model 93-20, Boston, MA) and a single junction reference electrode (Orion model 90-01) that connected to an Orion model 250A *p*H/temperature/mV meter (0.1-mV resolution, ±0.2 mV accuracy). Before the measurements were taken, a linear Ca^{2+} calibration (−19.4 - +20.2 mV; $r^2 = 0.984$) was prepared by measuring voltage differences for Ca^{2+} standards (0.09 - 2.9 mM). Readings were taken immediately after aliquot collection. Perfusate concentrations of Ca^{2+} were determined from the millivolt readings using the aforementioned calibration curve.

Nuclear Magnetic Resonance Methods

Two different types of NMR spectroscopy experiments were performed in this study: *in vivo* and high-resolution. The basic NMR phenomenon is at the heart of both methods, as is the basic technique: pulsed fourier transform NMR spectroscopy. A brief review of relevant, basic NMR principles is given in Appendix 1, which provides a foundation for Appendix 2, in which specific details are presented regarding NMR parameters in this study.

Statistical Analysis

Data are reported as mean ± SD. Average relative NMR metabolite values for different time points were compared first with a repeated-measures analysis of variance to determine if relative metabolite values appeared unchanged throughout time, *i.e.,* consistent with the null hypothesis. If the null hypothesis was rejected for a particular metabolite, data for that metabolite at each of the aforementioned time intervals were then subjected to a multiple-comparisons test. For this we used Bonferroni-corrected *t* tests, as in our previous studies.[15-18]

Results

Figure 1 shows the time dependence of $^{31}P/^{1}H$ NMR results. The most striking result in figure 1 is that during hypoxia, pretreatment with FBP results in almost total preservation of ATP and almost no increase in lactate. In the group pretreated with FBP, ATP levels were unchanged throughout the entire period of study (null hypothesis accepted, $P > 0.63$). Figure 1 also reveals that without pretreatment with FBP, hypoxia causes ATP and phosphocreatine to rapidly decrease to levels not detectable with NMR spectroscopy (*i.e.,* less than ≈0.5 mM). During hypoxia, in the group pretreated with FBP, phosphocreatine levels decreased more slowly than in the no treatment group ($P = 0.0001$, n = 3), although they became undetectable for both by the end of the hypoxia period (fig. 1B).

In slices not pretreated with FBP and in untreated slices, ATP returned to ≈50% of that in controls ($P < 0.0001$, n = 3 for both), and phosphocreatine returned to ≈80% of that in controls ($P < 0.0001$, n = 3 for both) after 60 min of hyperoxic recovery (figs. 1A and 1B). In all groups, pH_i decreased during hypoxia to ≈6.4 from 7.1 ($P < 0.0027$, n = 3). Similarly, in all groups, pH_i returned to control levels during hyperoxic recovery (fig. 1C). The rate of pH_i decrease and recovery was the same in all groups. NAA signal amplitudes were never seen to change; however, the lactate:NAA ratio increased from ≈1.0 to ≈7.0 in slices not treated with FBP (fig. 1D) and in slices posttreated with FBP. In contrast, pretreatment with FBP eliminated any increase in lactate (fig. 1D). Statistically, the lactate:NAA ratio was unchanged throughout the protocol (null hypothesis accepted, $P > 0.63$). (In NMR spectra from cerebrocortical slices, there is a small background lactate signal even in the control group. This is commonly attributed to the ≈50-μ - thick injury layer at the edge where slices were cut.[20,23])

Figure 2 shows representative cresyl violet - stained 20-μ - thick transverse sections from slices taken after 60 min of reperfusion. Shrunken nuclei and cell swelling can be found in sections taken from slices not pretreated with FBP. Qualitatively, average slice thickness after 60 min, as seen during light microscopy, was also noticeably greater in untreated and posttreated groups and was consistent with edema. Histologic features in sections from FBP-pretreated slices were not different from those in controls.

As can be seen in figure 3A, dynamic range limitations prevented our one-pulse, proton-decoupled ^{13}C NMR *ex vivo* spectra from showing glycolytic and tricarboxylic acid TCA cycle metabolites that might have incorporated the C2 label. The relatively high concentration of labeled glucose (5 mM), compared with micromolar concentra-

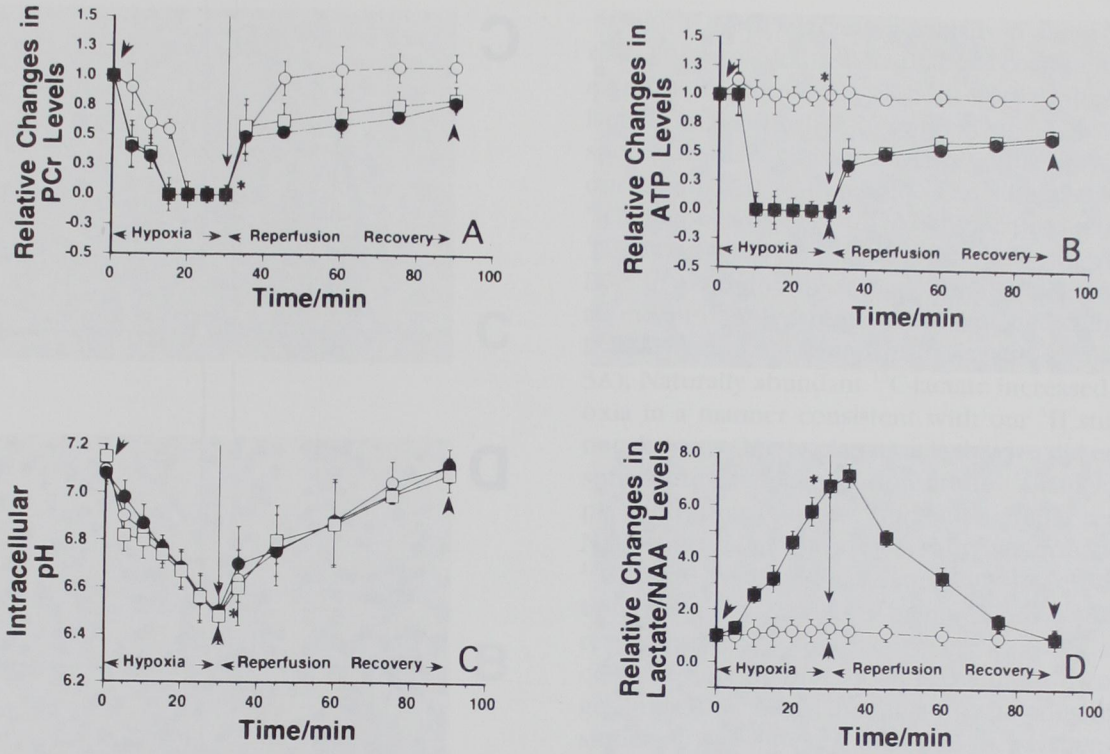

Fig. 1. Average nuclear magnetic resonance (NMR) metabolite determinations *versus* time during hypoxia studies. The *x* axis depicts the time in minutes since the beginning of the NMR experiment. Hypoxia and recovery periods are indicated. Data are shown as mean ± SD, from experiments with 2 mM of pretreatment with fructose-1,6-bisphosphate (FBP) (*open circles*), 2 mM of posttreatment with FBP (*filled circles*), and no FBP treatment (*open squares*) (n = 3 for each group). Representative NMR spectra (not shown) are of the same high quality as in our previous studies. For phosphocreatine (PCr) *(A)* and β-adenosine triphosphate (ATP) *(B)*, the *y* axis indicates the integrated NMR signal intensity normalized to its own control value. *(C)* The intracellular pH was obtained from σ, the inorganic phosphate (P_i)–PCr chemical shift, using the formula given in the text, as in our previous studies. *(D)* The lactate NMR peak area is normalized to the NMR peak area for *N*-acetyl-aspartate (NAA) in the same spectrum. In individual NMR experiments, in which amplifier gain was constant, NAA amplitudes were never seen to change. No relaxation time corrections were made to the spectra. Statistically significant data points (P = 0.0001, n = 3) are indicated by asterisks, and time points selected *a priori* for statistical comparison are indicated by arrows.

tions of metabolic intermediates, requires sophisticated NMR pulsing methods to suppress the large glucose peaks. The dynamic range problem is smaller in ^{13}C NMR spectra of perchloric acid (PCA) extracts (figs. 3B and 3C), because the perfusate is not present when obtaining extract spectra and the NMR signals are narrower in extracts. Some contribution from the perfusate might persist in extract spectra, however, because interstitial extracellular fluid is present in slices that are removed and frozen for the PCA extraction process.

Despite problems of dynamic range, figures 3B and 3C display a striking metabolic feature. A significant signal can be seen at 63.75 ppm in extract spectra of slices taken at the end of hypoxia but only in slices pretreated with FBP. This particular resonance peak is associated with the α,β-[1-^{13}C] carbon of F6P, shown schematically in figure 4, and its existence indicates that labeled glucose entered the PPP.[25–27] The [1-^{13}C]F6P signal was not seen when [2-^{13}C]glucose was metabolized aerobically, by untreated slices or by FBP-treated slices. Figure 4 shows that when [2-^{13}C]glucose gets metabolized to F6P via glycolysis, the label remains in the C2 position. When [2-^{13}C]glucose enters the PPP, however, the first step is decarboxylation at C1 of glucose. This causes the ^{13}C label, formerly at C2, to become a label at C1. At the end of the 30-min hypoxia period, for slices pretreated with FBP (n = 3), the average ratio of the [1-^{13}C]F6P signal to that for the β-anomer of [2-^{13}C]glucose was 0.09 ± 0.01. This corresponds to a [1-^{13}C]F6P concentration of ≈0.47 ± 0.03 mM. No detectable increases in lactate were seen in ^{13}C NMR spectra of PCA-extracted metabolites.

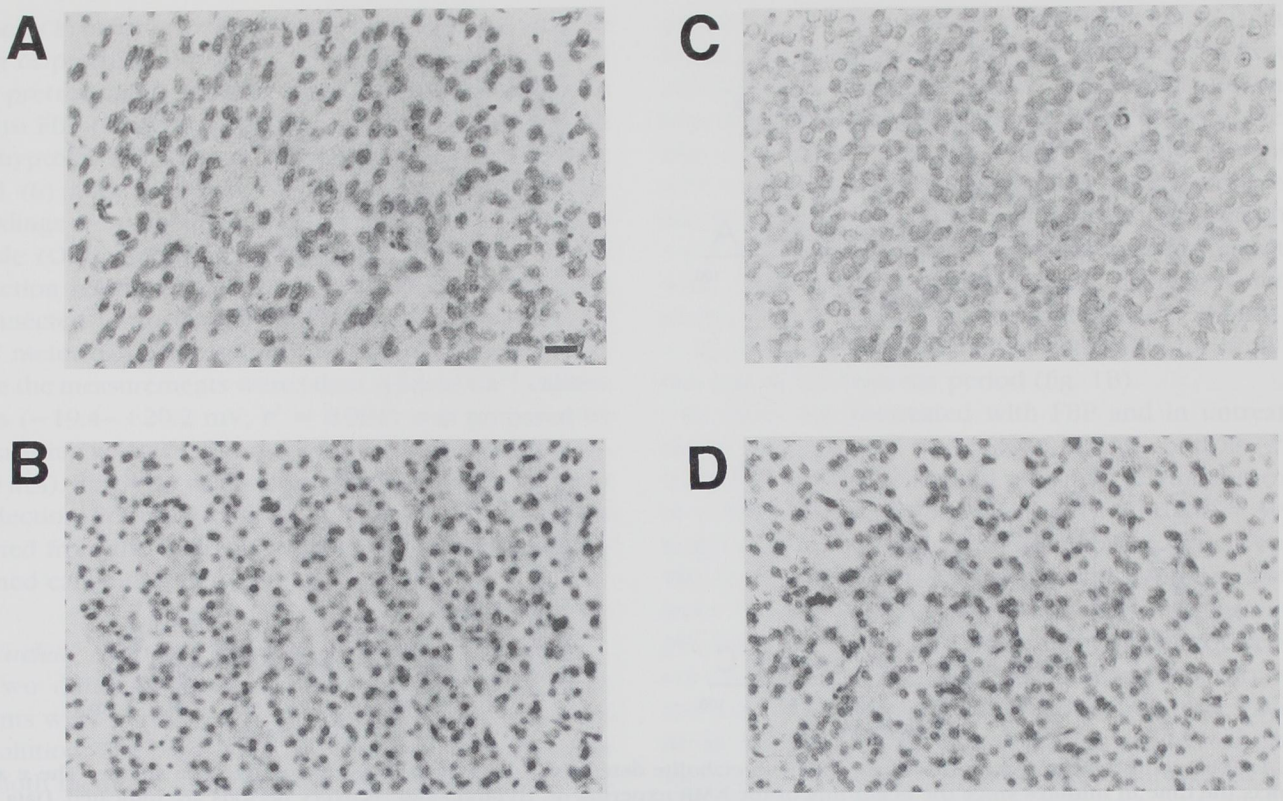

Fig. 2. Four micrographs of Nissl-stained slice sections from the following groups control (no insult) *(A)*; without pretreatment or posttreatment with fructose-1,6-bisphosphate (FBP) *(B)*; pretreatment with 2 mM FBP *(C)*, and posttreatment with 2 mM FBP *(D)*. Random slices were taken at the end of the 60 min of reperfusion recovery in normoxic artificial cerebrospinal fluid. Qualitatively, pretreatment with FBP prevented oxygen deprivation–induced shrinking of Nissl-stained neuronal nuclei *(C)* and cell swelling seen as vacuolization around nuclei *(B and D)*. The scale bar (=20 μm) is the same for all micrographs.

Measurements of free, ionized calcium concentrations in the perfusate are given in table 1. Addition of FBP to perfusate obtained from the Cell Culture Facility at University of California, San Francisco caused an ≈17% decrease in the calcium concentration of the input perfusate. Aliquots of artificial cerebrospinal fluid taken from the NMR tube after no-flow hypoxia (with all slices still in place, before reflow was started), however, showed that hypoxia led to ≈50–60% decreases in calcium in the surrounding perfusate. As can be seen in table 1, calcium concentrations in aliquots taken at the end of hypoxia were identical for the FBP pretreatment and no treatment groups.

Discussion

As in earlier studies that found FBP to be protective,[1–9] acute energy failure in cerebrocortical tissue during rapid-onset hypoxia was substantially ameliorated by FBP pretreatment, as was the rise in tissue lactate concentrations. FBP-induced reductions in lactate production during hypoxia have been observed previously.[4–6,28,29] It is possible that FBP enters cells, causes feedback inhibition of phosphofructokinase, and retards or arrests glycolysis. It is nevertheless unusual that, in slices pretreated with FBP, pH_i decreased during hypoxia without an increase in lactate. Where are the hydrogen ions coming from if not from lactate? It is probable that most hydrogen ions come from ATP hydrolysis[30] and that those coming from lactate are a small percentage of the total hydrogen ion pool. This would be consistent with the findings of Hida *et al.*, who showed that intracellular acidosis is not always coupled to increases in intracellular lactate.[31] The simultaneous preservation of ATP and increase in hydrogen ions in our severely hypoxic brain slices remain unexplained, however.

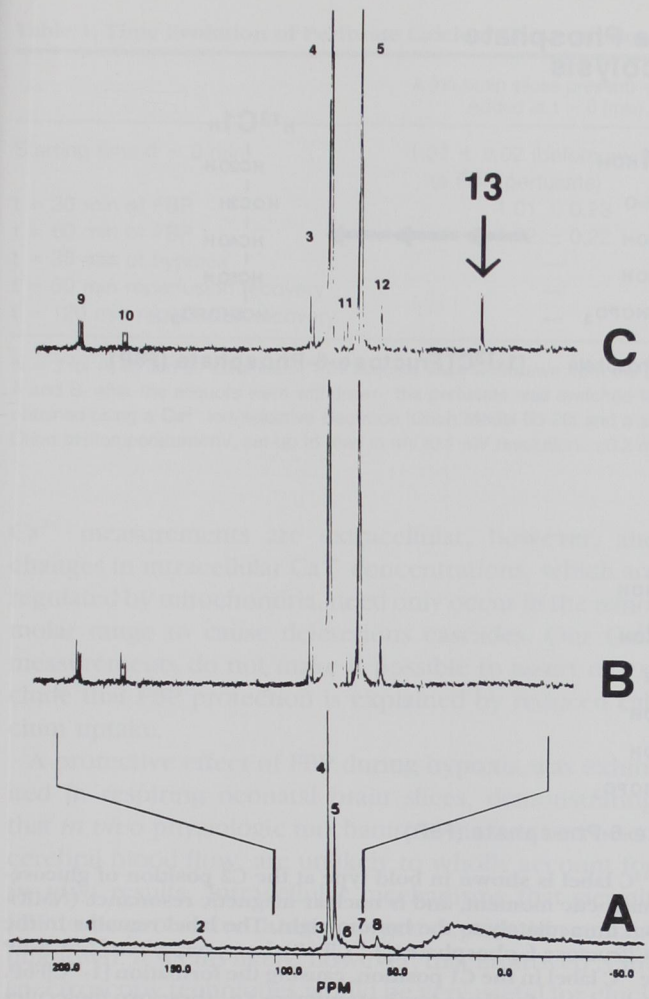

Fig. 3. From bottom to top: *(A)* Representative *ex vivo* proton-decoupled ^{13}C nuclear magnetic resonance (NMR) spectrum of respiring neonatal rat brain slices perfused with hyperoxic artificial cerebrospinal fluid that contained 5 mM [2-^{13}C]glucose but no fructose-1,6-bisphosphate (FBP). Labeled glucose was administered for 60 min just before hypoxia. The NMR data acquisition time was 30 min. *(B and C)* Representative *in vitro* high resolution proton-decoupled ^{13}C NMR spectrum of perchloric acid extracts. Perfused slices were removed from the NMR tube and frozen at the end of 30 min of hypoxia. Slices were pretreated with 5 mM [2-^{13}C]glucose during the 60-min period just before hypoxia. In *B,* no pretreatment with FBP was administered. In *C,* conditions were the same as in *B,* except that slices were also pretreated with 2 mM FBP during the 60-min period just before hypoxia. Only in C does one see resonance (13) at 63.75 ppm. Assignment of resonance is as follows: (1) CEO, carbonyl carbons; (2) BCH_2ECH-$BCHECH_2B$, fatty acid side chains; (3) β-[C3], β-[C5] glucose; (4) β-[C2]glucose; (5) α-[C2]glucose; (6) C2 lactate; (7) GPC, choline; (8) choline, creatine, phosphocreatine, glutamine, glutamate, aspartate, and glutathione; (9) and (10), C1 glucose (contaminants from C2-glucose sample); (11) not identified (from C2-glucose); (12) α-[C3]glucose; and (13) C1 fructose-6-phosphate.

Our ^{13}C NMR extract spectra from slices pretreated with FBP provided results that are consistent with our *ex vivo* ^{1}H NMR results. In both studies, there were no lactate increases after hypoxia. Our ^{13}C NMR extract spectra results for untreated slices differ, however, from our *ex vivo* ^{1}H NMR results. The administration of [2-^{13}C]glucose did not result in hypoxic production of [1,2-^{13}C]lactate and [2,3-^{13}C]lactate in slices not treated with FBP. In preliminary *ex vivo* ^{13}C NMR studies of naturally abundant ^{13}C, we noted small but detectable control levels of naturally abundant ^{13}C-lactate (peak no. 6, fig. 3A). Naturally abundant ^{13}C-lactate increased with hypoxia in a manner consistent with our ^{1}H studies (data not shown). One explanation is that we did not provide sufficient time for migration of the ^{13}C label. In principle, perfusion with [2-^{13}C]glucose should result in ^{13}C NMR spectra of PCA extracts showing formation of [1,2-^{13}C]lactate and [2,3-^{13}C]lactate, with the resonance positions for C1, C2, and C3 being 183, 69, and 20 ppm, respectively.[24-26] Our slices were exposed to ^{13}C glucose for only 60 min, however. Studies by others suggest that this might not have been enough time for sufficient quantities of the label to advance to lactate through glycolysis.[32] It is possible that longer exposure to ^{13}C-labeled glucose might result in sufficient ^{13}C-labeled lactate. Long exposures involve more extensive migrations of the ^{13}C-label, however, which sometimes causes difficulty in the interpretation of measurements. Experiments with ^{13}C-labeled FBP might be helpful, but the same experimental challenges remain that were present in our ^{13}C-labeled glucose studies — overcoming the dynamic range issue and having enough time for sufficient label migration through metabolic pathways.

Because diverse organ systems appear to benefit from pretreatment with FBP during oxygen deprivation, it has been postulated that the primary action of FBP is metabolic and that during oxygen deprivation FBP improves ATP supply *versus* demand.[4-6] A possible mechanism by which FBP sustains ATP levels is by acting as a metabolic substrate that stimulates the PPP, causing increased formation of triose phosphates.[33] Bader-Gofer *et al.*[25] previously pointed out that in ^{13}C NMR studies C1-labeled glucose was useful for avoiding the PPP, whereas C2-labeled glucose was useful for probing it. Similarly, Ben-Yoseph *et al.*[34] showed that the use of isotopically substituted D-[1,6-^{13}C;6,6-$^{2}H2$]glucose can be used to measure relative activities of PPP when used in conjunction with microdialysis. It has been demonstrated *in vitro* that FBP activates the nonoxidative arm

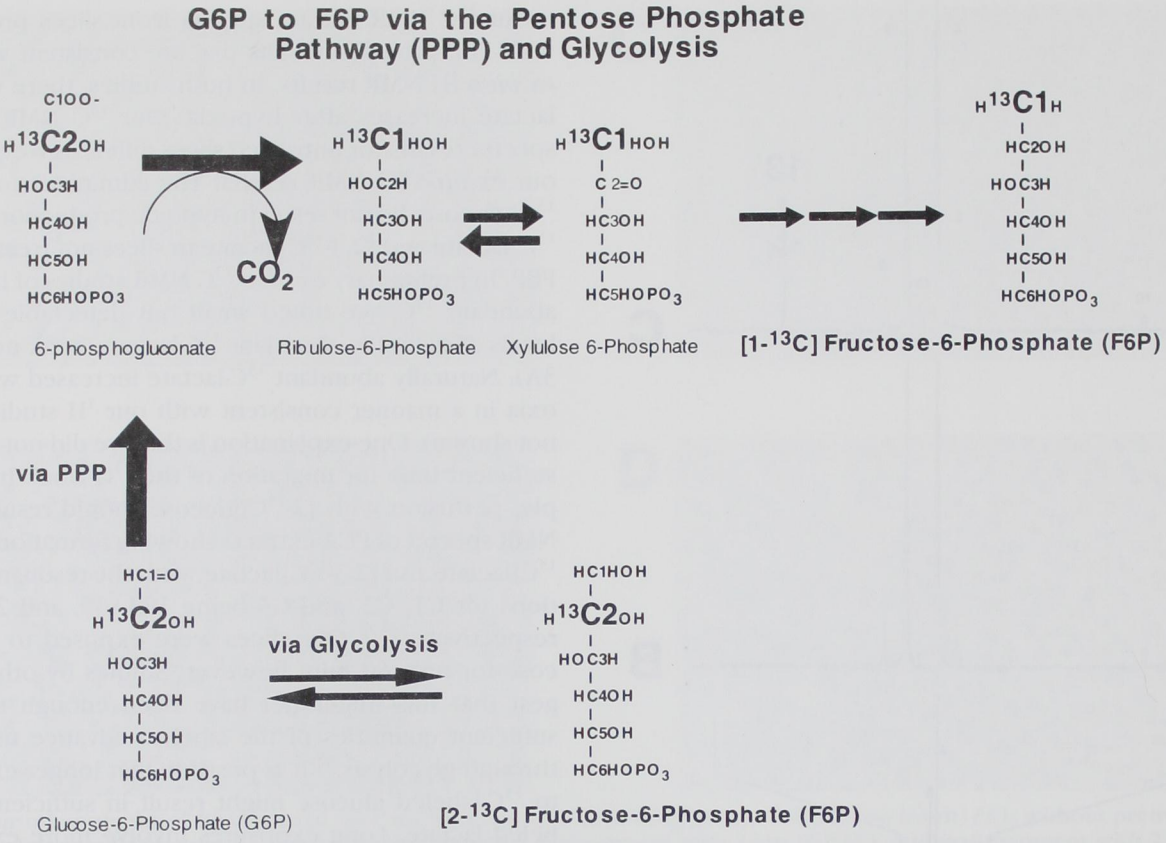

Fig. 4. This schematic diagram begins at the bottom left, where a ^{13}C label is shown in bold type at the C2 position of glucose-6-phosphate ([2-^{13}C]G6P). Naturally abundant carbon, ^{12}C, has no magnetic moment, and is nuclear magnetic resonance (NMR)-invisible. The position of ^{13}C in the next step of glycolysis is shown immediately to the bottom right. The label remains in the C2 position after phosphoglucose isomerase converts G6P into [2-^{13}C]fructose-6-phosphate ([2-^{13}C]F6P); however, when [2-^{13}C]G6P traverses the pentose phosphate pathway, decarboxylation puts the ^{13}C label in the C1 position, causing the formation [1-^{13}C]F6P. Distinctly different chemical shifts characterize the ^{13}C-NMR resonance peaks for these two isotopomers, *i.e.,* these two molecules that are identical except for the location of an isotope label. Measured relative to the chemical shift for [2-^{13}C]glucose at 74.1 ppm, the chemical shift for the ^{13}C resonance of [1-^{13}C]F6P is at 63.75 ppm, whereas that for [2-^{13}C]F6P is at 76–82.59 ppm. Therefore, it is possible to distinguish F6P formed *via* the pentose phosphate pathway from F6P formed by glycolysis.

of the PPP,[35] which interconverts various sugars without generating NADPH from nicotinamide-adenine dinucleotide phosphate and converts glucose to triose phosphates with no expenditure of ATP. Triose phosphates from the PPP must still go through the TCA cycle, however, if full ATP production is to occur. Furthermore, during hypoxia, one would expect an increase in triose phosphates to lead to an increase in lactate; therefore, an FBP-induced increase in PPP-related F6P does not entirely explain FBP-induced ATP conservation. Additionally, the PPP is more active in immature brain, and the results, which were obtained in tissue from 7-day-old rats, might be unique to the neonate.

Alternative hypotheses of FBP protection have included calcium chelation, free-radical scavenging, and protease inhibition.[33,35–37] Hassinen *et al.,* suggested that FBP protection in perfused hearts came primarily from extracellular calcium chelation.[35] They also found redox preservation, however, which must have resulted from other mechanisms. In two previous studies using intracellular fluorescent calcium indicators on astrocytes and brain slices, FBP was found to prevent hypoxia-induced increases in extracellular glutamate and intracellular Ca^{2+}, and hypoxia-induced depletion of ATP.[7,10] Although we found that the addition of FBP to the normal perfusate caused an ≈17% decrease in Ca^{2+}, free calcium in the perfusate at the end of no-flow hypoxia was unchanged by pretretament with FBP. Such

Table 1. Time Evolution of Perfusate Calcium Concentrations

	A (no brain slices present) + FBP Added at t = 0 (mM)	B (brain slices present) + FBP Added at t = 0 (mM)	C (brain slices present); No FBP Added at t = 0 (mM)
Starting time (t = 0 min)	1.21 ± 0.02 (before switching to FBP perfusate)	1.23 ± 0.03 (before switching to FBP perfusate)	1.21 ± 0.02
t = 30 min of FBP	1.01 ± 0.23	1.02 ± 0.22	—
t = 60 min of FBP	1.02 ± 0.22	1.02 ± 0.20	—
t = 30 min of hypoxia	—	0.57 ± 0.03	0.56 ± 0.02
t = 60 min reperfusion recovery	—	0.81 ± 0.03	0.75 ± 0.06
t = 120 min reperfusion recovery	—	1.21 ± 0.03	1.24 ± 0.04

N = 3 for A, B, and C. Volumes of 1 ml aliquots were withdrawn from the bottom of the NMR chamber at indicated times, at temperature = 37°C. In columns A and B, after the aliquots were withdrawn, the perfusate was switched to one having 2 mM FBP, at starting time (t = 0 min). All Ca^{2+} measurements were obtained using a Ca^{2+} ion-selective electrode (Orion Model 93-20) and a single junction reference electrode (Orion Model 90-01) connected to a Model 250A Orion *p*H/temperature/mV, set up to read in mV (0.1 mV resolution, ±0.2 mV accuracy).

Ca^{2+} measurements are extracellular, however, and changes in intracellular Ca^{2+} concentrations, which are regulated by mitochondria, need only occur in the nanomolar range to cause deleterious cascades. Our Ca^{2+} measurements do not make it possible to assert or exclude that FBP protection is explained by reduced calcium uptake.

A protective effect of FBP during hypoxia was exhibited in respiring neonatal brain slices, demonstrating that *in vivo* physiologic mechanisms, such as increased cerebral blood flow, are unlikely to wholly account for *in vivo* results. Intracellular mechanisms that permit FBP to be protective during oxygen deprivation remain unknown. It seems likely, however, that improved NMR spectroscopy techniques would be very useful for elucidating metabolic changes during studies of this type.

Appendix 1: Brief Review of Basic Issues in *Ex Vivo* and High-Resolution NMR Spectroscopy

For both types of spectroscopy, conditions for observing the NMR phenomenon are established in steps.[38–40] First, one applies a strong, constant magnetic field, typically 2–20 T in strength. (For comparison, the magnitude of the earth's magnetic field is ≈50 μT.) The magnetic field causes all magnetic dipoles (objects behaving like compass needles) to precess about the direction of the applied field, a phenomenon called Larmor precession, at a frequency (called the Larmor frequency) that is the product of three factors: a universal constant, the strength of the magnetic field, and the strength of the magnetic moment. Nuclear magnetic moments are typically ≈1,000 times smaller than the magnetic moment of the electron or magnetic moments of atoms and molecules. At 1 T, Larmor frequencies for ^{1}H, ^{31}P, and ^{13}C are, respectively, 42.576, 17.236, and 10.705 MHz. At 4.7 and 11.75 T, Larmor frequencies for ^{1}H are, respectively, 200 and 500 MHz.

The Larmor frequencies calculated from a knowledge of the applied field apply only to isolated dipole moments, *i.e.,* isolated ^{1}H, ^{31}P, and ^{13}C nuclei, floating alone in space, experiencing only the applied magnetic field. Nuclei are not alone, however; they are surrounded by atomic electrons, the rest of the parent molecule, and numerous other molecules. The static magnetic fields used in NMR spectrometers are uniform to approximately 1 part in 10^{8}. Magnetic fields generated within a molecule by orbiting electrons, however, add to the applied magnetic field, changing the total magnetic field and final precession frequency at a particular molecular position, typically by several ppm. Consequently, within a single molecule, different electronic environments can be experienced by chemically different nuclei of the same type. Such is the case for the three ^{31}P nuclei in ATP. Each has a different Larmor frequency (by ≈5–14 ppm) that is clearly distinguishable with NMR spectroscopy.

In the second step of NMR spectroscopy, a rapidly rotating magnetic field is applied to the sample for a short period, typically tens to hundreds of microseconds, by a radiofrequency excitation coil. Magnetic moment transitions occur if and only if the frequency of the applied radiofrequency field is the same as the nuclear precession frequency. This phenomenon is known as nuclear magnetic resonance. The magnetic moment transitions absorb energy from the radiofrequency magnetic field, and this is sensed by a detection coil. Absorption signals occur at resonance frequencies, *i.e.,* at radiofrequencies corresponding to the different precession frequencies of chemically distinct nuclei, for all molecules in the sample. Thus, NMR spectroscopy is absorption spectroscopy, and the shift in resonance frequencies caused by different chemical environments is called the chemical shift.

The radiofrequency detection coil is often physically the same as the radiofrequency excitation coil. (Circuitry to the coil, however, must then be changed rapidly from excitation circuitry to detection circuitry.) Although excitation by a radiofrequency pulse is typically centered at the Larmor frequency of a particular nucleus, there are band widths to the excitation (and detection), and these are made wide enough to include all resonance frequencies of interest. For ^{31}P spectroscopy of biologic tissue, sharp absorption signals can be detected at separate frequencies (over a range of ≈30 ppm), *e.g.,* for phosphoenthanolamine, sugar phosphates (*e.g.,* FBP, F6P, G6P), P_i, phosphodiesters, phosphocreatine, and the α, β, and γ ^{31}P nuclei in ATP.

We have mentioned that different molecular positions for particular nuclei are often uniquely identifiable. Such is the case for P_i, which exists primarily as one of two species at physiologic *p*H: $H_2PO_4^-$ (acid) $\leftrightarrow H^+ + HPO_4^{--}$ (base), with $pK_a \approx 6.75$. The chemical shift of the ^{31}P resonance in $H_2PO_4^-$ is ≈ 2 ppm different from the chemical shift of the ^{31}P resonance in HPO_4^{--}. The ^{31}P nucleus experiences a different magnetic field in the two P_i species because of the absence or presence of a single proton. For a particular P_i molecule, protonation and deprotonation occur so rapidly that the ^{31}P nucleus experiences both species many times during the period of NMR resonance detection (milliseconds). The ^{31}P nucleus of P_i in this situation is said to be in rapid exchange between the two species, and the measured resonance frequency for the ^{31}P nucleus turns out to be the weighted average of the resonance frequencies for the two P_i species. The weights, which are the ratios of the two phosphate species to total P_i, uniquely relate to the chemical shift measured for P_i. Theoretically, the ratio of the two phosphate species also relates uniquely to pH_i *via* the Henderson–Hasselbalch equation. Thus, pH_i and the measured P_i chemical shift are linked, as explained in Appendix 2, in which an explicit formula is given.

After a radiofrequency pulse is applied to a sample, one detects the NMR signal for a fixed period, during which it decays exponentially. The measured signal is called a free induction decay (FID). Many FIDs are summed and averaged to eliminate contributions from random fluctuations (noise). After an average FID has been obtained, a fourier transform is performed to obtain the NMR spectrum, a plot of NMR signal amplitude *versus* frequency. (The process is analogous to that used for power analysis of electroencephalographic spectra—in which electroencephalographic amplitudes are recorded for time epochs and fourier transformation is used to get amplitudes *vs.* frequency.) Averaging FIDs is an important method of increasing signal-to-noise ratios in NMR spectra. Typically, it takes a few minutes to accumulate the necessary number of FIDs, and one waits ≥ 1 s after a radiofrequency pulse before providing the next one. A long interpulse delay gives nuclei time to relax after radiofrequency excitation. Because resonance frequencies are different among nuclei, one can perform a radiofrequency excitation and FID collection for ^{31}P (or ^1H) during the time that ^1H (or ^{31}P) nuclei are relaxing if one has appropriate electronic equipment and is able to perform adequate computer tracking of the data. It is thus possible to obtain NMR spectra for two or more nuclei during the same 5-min period required to obtain a spectrum for only one. This is known as interleaved spectroscopy. The previous section is general and limited; omitted are technical descriptions of phase, a quantity that describes the frequency coherence of detected signals, and quadrature detection, a method that facilitates the correct assignment of frequencies relative to a reference frequency. Interested readers are referred to comprehensive texts.[38–40]

In high-resolution NMR spectroscopy, nuclei have parent molecules that are freely mobile in dilute solutions. We used high-resolution NMR spectroscopy to study metabolites extracted from brain slices. We obtained the metabolites by rapidly freezing the slices in liquid nitrogen, pulverizing the frozen tissue to a powder, and dissolving it in cold perchloric acid solution to preserve metabolites and inactivate enzymes. In brain slice studies, it is very convenient to obtain and freeze the tissue quickly. In addition, higher concentrations of compounds of interest can be made after lyophilizing solutions with extracts. With high-resolution NMR spectroscopy, one destroys the cells but detects all atomic nuclei because all molecules are freely mobile in solution.

The situation for *in vivo* NMR spectroscopy is different. *In vivo,* molecules are often bound or partitioned in macromolecular structures. As texts explain, large macromolecules and small ones bound to them move and tumble more slowly, causing broader NMR signals from reporting nuclei. The NMR signal intensity, or area under a signal's curve, is proportional to the concentration of the signal (assuming that FIDs are acquired with long interpulse delays that lead to full relaxation). For a fixed concentration, *i.e.,* for a fixed NMR signal intensity, the height of an NMR signal diminishes as it widens. Macromolecular interactions can thus cause the height of a signal (amplitude) to become so small that it is no larger than the signal amplitude for random noise. In such cases, the signal is no longer detectable with NMR spectroscopy. With *in vivo* NMR spectroscopy, cells are not destroyed, but line broadening causes fewer nuclei to be detectable by NMR, and it causes some detectable signals to overlap with others.

Appendix 2: Details of Methods We Used for *Ex Vivo* and High-Resolution Nuclear Magnetic Resonance Spectroscopy

Ex Vivo

Interleaved ^{31}P and ^1H spectra were obtained on a Nalorac Quest Model 4400 (Martinez, CA) 4.7-T NMR instrument, operating at 81 and 200 MHz, respectively, using methods described previously.[17] The 20-mm NMR tube containing 80 slices was positioned inside a custom-made probe. The probe had a 24-mm (outer diameter) Helmholtz coil on a Pyralux flexible composite (Du Pont Electronics, Towanda, PA) that was tuned to ^1H. An inner four-turn 23-mm (outer diameter) solenoidal coil was tuned to ^{31}P. Each acquisition consisted of 2,048 complex data points for both ^{31}P and ^1H. Time-sharing was such that it took 0.84 s for a single ^{31}P acquisition and 1.27 s for a single ^1H acquisition. Individual spectra for ^{31}P and ^1H were generated after 120 acquisitions in quadrature phase detection mode. The spectral width was $\pm 4{,}000$ Hz. Nuclear magnetic resonance signal intensities for each metabolite were determined by numerical integration of optimal computer fits to corresponding NMR resonance peaks (Nalorac Quest Model 4400 Curve Fitting Program; and MacFID Curve Fitting Program, Tecmag Inc., Bellaire, TX).

^{31}P Magnetic excitation was typically *via* one radiofrequency pulse of ≈ 30 μs, causing a tip angle of $\approx 45°$. The broad ^{31}P phospholipid hump was subtracted using a convolution difference method having a 500-Hz exponential filter. ^{31}P Metabolite concentrations were measured relative to corresponding signal peak areas in the control run (time = 0 min) and expressed as $[\text{Peak area}]_{\text{time}=t}/[\text{Peak area}]_{\text{time}=0}$. Relative ATP levels were determined from the β-ATP peak at 16.3 ppm. It is apparent from prior T_1 measurements by others[41] that pulse conditions do not allow observation of fully relaxed signals. For example, the following T_1 values have long been known for 4.7 T[41]: ≈ 3.5 s for phosphocreatine; ≈ 3.8 s for phosphomonoesters (PME); ≈ 2.6 s for P_i; and ≈ 1.3 s for β-ATP. Acquisition conditions were the same for all experiments, however. If one assumes, as others do, that T_1 values do not change, then changes in NMR signal intensity in any metabolite are directly proportional to changes in the concen-

tration of that metabolite. Therefore, no correction for saturation is needed when measuring relative changes of a particular brain slice metabolite.[42] Intracellular *p*H was calculated from the P_i–phosphocreatine chemical shift difference, σ, using an equation that was tested by several groups and ultimately refined[43]: $pH_i = 6.75 + \log([\sigma - 3.27]/[5.69 - \sigma])$.

Spin-echo ^{1}H NMR spectroscopy experiments were initiated with a 100-ms low-power presaturation pulse centered on the water resonance. A 136-ms spin-echo delay (TE) for refocusing pulses permitted substantial discrimination against more rapidly relaxing lipid signals near the 1.32-ppm lactate peak. ^{1}H Magnetic excitation pulses required a 50-watt amplifier and typically occurred via a radiofrequency pulse of ≈196 μs duration, causing a tip angle of 90°. A Lorentzian-to-Gaussian transformation for each ^{1}H spectrum was performed by multiplying by a −12-Hz exponential and a 7-Hz Gaussian.

Ex vivo proton-decoupled ^{13}C NMR spectra of perfused brain slices were also obtained at 4.7 T during special studies in which there was administration of either [2-^{13}C] glucose or normal glucose. (Proper determination of low-concentration metabolite changes after [2-^{13}C]glucose administration requires a knowledge of background signal intensities occurring from naturally abundant ^{13}C [≈1.1% of all carbon nuclei].) *Ex vivo* ^{13}C NMR studies were performed using a custom-built probe tuned to 50.32 MHz. Ten minutes was required to obtain one spectrum. Each 10-min acquisition consisted of 4,096 complex data points, obtained in quadrature phase detection mode. The spectral width was ±12,000 Hz. ^{13}C Magnetic excitation was typically from one radiofrequency pulse of ≈70 μs, causing a tip angle of 45°. An exponential filter of 12–15 Hz was used to reduce noise in the spectra. A WALTZ-16 scheme was used during acquisitions for broadband proton decoupling. Studies of naturally abundant ^{13}C metabolites required the addition of three 10-min acquisitions.

High-resolution ^{13}C NMR Spectroscopy of Extracted Metabolites

Additional separate studies with ^{13}C-enriched glucose were conducted for NMR studies of extracted metabolites. In these, all 80 brain tissue slices (3.2 g wet weight) were removed just before hypoxia or at the end of the 30-min hypoxia period and were immediately frozen in liquid nitrogen. After perchloric acid extraction, proton-decoupled ^{13}C NMR spectra were obtained with an 11.75-T GN500 instrument (Brucker Instruments, Billerica, MA) operating at 126 MHz. In the extraction procedure, frozen slices were ground into a fine powder in a cryo-cooled mortar and then dissolved in a 1.0 N $HClO_4$ solution containing 20 mM edetic acid, using a 1:2 (weight:volume) ratio. Separation of cell debris from perchloric acid extracts was accomplished at 4°C by 10 min of centrifugation at 15,000 rpm (Sorvall Refrigerated Centrifuge, IL). The H of the perchloric acid extract was adjusted to ≈7 using 1 N KOH. Solutions were subsequently frozen in liquid nitrogen and lyophilized using a Labconco freeze-dryer (Fischer Scientific, Fremont, Newton, CT). Immediately before high-resolution NMR studies, the freeze-dried perchloric acid extracts were dissolved in 0.5 ml deuterium oxide (D_2O) and transferred to a 5-mm (outer diameter) NMR tube.

Data acquisitions for high resolution ^{13}C experiments were accumulated in 4-h blocks. Typically, four to six blocks were summed to obtain improved signal-to-noise ratios. Each high-resolution NMR acquisition consisted of 4,096 complex data points, obtained in quadrature phase detection mode. The spectral width was 30,000 Hz. ^{13}C Magnetic excitation was typically one radiofrequency pulse of ≈20 μs in duration, causing a tip angle of 45°. As in *ex vivo* NMR studies, an exponential filter of 3–7 Hz was used to reduce spectral noise, and a WALTZ-16 scheme was used for broadband proton decoupling. Chemical shifts were referenced to resonance peaks for [β-C2]glucose at 74.1 ppm.[25–27]

References

1. Markov AK, Oglethorpe NC, Grillis M, Neely WA, Hellems HK: Therapeutic action of fructose-1,6-diphosphate in traumatic shock. World J Surg 1983; 7:430–6

2. Sun JX, Farias LA, Markov AK: Fructose 1–6 diphosphate prevents intestinal ischemic reperfusion injury and death in rats. Gastroenterology 1990; 98:117–26

3. Farias LA, Smith EE, Markov AK: Prevention of ischemic-hypoxic brain injury and death in rabbits with fructose-1,6-diphosphate. Stroke 1990; 21:606–13

4. Gregory GA, Yu AC, Chan PH: Fructose-1,6-bisphosphate protects astrocytes from hypoxic damage. J Cereb Blood Flow Metab 1989; 9:29–34

5. Sola A, Berrios M, Sheldon RA, Ferriero DM, Gregory GA: Fructose-1,6-bisphosphate after hypoxic ischemic injury is protective to the neonatal rat brain. Brain Res 1996; 741:294–9

6. Kelleher JA, Chan PH, Chan TYY, Gregory GA: Energy metabolism in hypoxic astrocytes: Protective mechanism of fructose-1,6-bisphosphate. Neurochem Res 1995; 20:785–92

7. Bickler PE, Kelleher JA: Fructose-1,6-bisphosphate stabilizes brain intracellular calcium during hypoxia in rats. Stroke 1992; 23:1617–22

8. Kuluz JW, Gregory GA, Han Y, Dietrich WD, Schleien CL: Fructose-1,6-bisphosphate reduces infarct volume after reversible middle cerebral artery occlusion in rats. Stroke 1993; 24:1576–83

9. Kelleher JA, Gregory GA, Chan PH: Effect of FBP on glutamate uptake and glutamine synthetase activity in hypoxic astrocyte cultures. Neurochem Res 1994; 19:209–15

10. Bickler PE, Buck LT: Effects of fructose-1,6-bisphosphate on glutamate release and ATP loss from rat brain slices during hypoxia. J Neurochem 1996; 67:1463–8

11. LeBlanc MH, Farias LA, Evans OB, Vig V, Smith EE, Markov AK: Fructose-1,6-bisphosphate, when given immediately before reoxygenation, or before injury, does not ameliorate hypoxic ischemic injury to the central nervous system in the newborn pig. Crit Care Med 1991; 19:75–83

12. LeBlanc MH, Farias LA, Markov AK, Evans OB, Smith B, Smith EE, Brown EG: Fructose-1,6-diphosphate, when given five minutes after injury, does not ameliorate hypoxic ischemic injury to the central nervous system in the newborn pig. Biol Neonate 1991; 59:98–108

13. LeBlanc MH, Parker CC, Vig V, Smith EE, Brown EG: Fructose-1,6-bisphosphate does not ameliorate hypoxic ischemic injury to the central nervous system in the newborn pig. Crit Care Med 1992; 20:1309–14

14. Clarke DD, Sokoloff L: Circulation and energy metabolism of the brain, Basic Neurochemistry. 5th edition. Edited by Siegel GJ, Agranoff BW, Albers RW, Molinoff PB. New York, Raven Press, 1993, p 654

15. Espanol MT, Litt L, Yang GY, Chang LH, Chan PH, James TL, Weinstein PR: Tolerance of low intracellular pH during hypercapnia by rat cortical brain slices: A $^{31}P/^{1}H$ NMR study. J Neurochem 1992; 59:1820–8

16. Espanol MT, Xu Y, Litt L, Yang GY, Chang LH, James TL, Weinstein P, Chan PH: Modulation of glutamate-induced intracellular energy failure in neonatal cerebral cortical slices by kynurenic acid, dizocilpine, and NBQX. J Cereb Blood Flow Metab 1994; 14:269–78

17. Espanol MT, Xu Y, Litt L, Chang L-H, James TL, Weinstein PR, Chan PH: ^{19}F NMR calcium changes, edema, and histology in neonatal rat brain slices during glutamate toxicity. Brain Res 1994; 647:172–6

18. Espanol MT, Litt L, Chang LH, James TL, Weinstein PR, Chan PH: Adult rat brain-slice preparation for nuclear magnetic resonance spectroscopy studies of hypoxia. ANESTHESIOLOGY 1996; 84:201–10

19. Chan PH, Fishman RA: Brain edema: Induction in cortical slices by polyunsaturated fatty acids. Science 1978; 201:358–60

20. Dingledine R: Brain Slices. New York, Plenum Press, 1984

21. Brain Slices in Basic and Clinical Research. Edited by Shurr A, Rigor BM. Boca Raton, CRC Press, 1995

22. Whittingham TS, Lust WD, Christakis DA, Passonneau JV: Metabolic stability of hippocampal slice preparations during prolonged incubation. J Neurochem 1984; 43:689–96

23. Hasegawa K, Litt L, Espanol MT, Gregory GA, Sharp FR, Chan PH: Effects of neuroprotective dose of fructose-1,6-bisphosphate on hypoxia-induced expression of c-fos and hsp70 mRNA in neonatal rat cerebrocortical slices. Brain Res 1997; 750:1–10

24. Tecoma ES, Monyer H, Goldberg MP, Choi DW: Traumatic neuronal injury in vitro is attenuated by NMDA antagonists. Neuron 1989; 2(6):1541–5

25. Badar-Goffer RS, Ben-Yoseph O, Bachelard HS, Morris PG: Neuronal-glial metabolism under depolarizing conditions: A ^{13}C NMR study. Biochem J 1992; 282:225–30

26. Schrader MC, Eskey CJ, Simplaceanu V, Ho C: A carbon-13 nuclear magnetic resonance investigation of the metabolic fluxes associated with glucose metabolism in human erythrocytes. Biochim Biophys Acta 1993; 1182:179–88

27. Schrader MC, Simplaceaneu V, Ho C: Measurement of fluxes through the pentose phosphate pathway in erythrocytes from individuals with sickle cell anemia by carbon-13 nuclear magnetic resonance spectroscopy. Biochim Biophys Acta 1993; 1182:162–78

28. Gregory GA, Welsh FA, Yu AC, Chan PH: Fructose-1,6-bisphosphate reduces ATP loss from hypoxic astrocytes. Brain Res 1990; 516:310–2

29. Gobbel GT, Chan TY, Gregory GA, Chan PH: Response of cerebral endothelial cells to hypoxia: Modification by fructose-1-6-bisphosphate but not glutamate receptor antagonists. Brain Res 1994; 653:23–30

30. Alberti KG, Cuthbert C: The hydrogen ion in normal metabolism: A review, Metabolic Acidosis, Ciba Foundation Symposium 87. Edited by Porter R, Lawrenson G. London, Pitman Books, 1982, pp 1–19

31. Hida K, Suzuki N, Kwee IL, Nakada T: pH-lactate dissociation in neonatal anoxia: Proton and ^{31}P NMR spectroscopic studies in rat pups. Magn Reson Med 1991; 22:128–32

32. Gruetter R, Novotny EJ, Boulware SD, Mason GF, Rothman DL, Shulman GI, Prichard JW, Shulman RG: Localized ^{13}C NMR spectroscopy in the human brain of amino acid labeling from D-[1-^{13}C]glucose. J Neurochem 1994; 63:1377–85

33. Tavazzi B, Starnes JW, Lazzarino G, Di Pierro D, Nuutinen EM, Giardina B: Exogenous fructose-1,6-bisphosphate is a metabolizable substrate for the isolated normoxic rat heart. Basic Res Cardio 1992; 87:280–9

34. Ben-Yoseph O, Camp DM, Robinson TE, Ross BD: Dynamic measurements of cerebral pentose phosphate pathway activity *in vivo* using [1,6-^{13}C2,6,6-^{2}H2]glucose and microdialysis. J Neurochem 1995; 64:1336–42

35. Hassinen IE, Nuutinen EM, Ito K, Nioka S, Lazzarino G, Giardina B, Chance B: Mechanism of the effect of exogenous fructose 1,6-bisphosphate on myocardial energy metabolism. Circulation 1991; 83:584–93

36. Orstan A, Gafni A: Inhibition of proteinase K by phosphorylated sugars. Biochem Int 1991; 25:657–62

37. Fukushima E, Roeder SBW. Experimental Pulse NMR: A Nuts and Bolts Approach. Reading, Addison-Wesley Advanced Book Program, 1981

38. Martin ML, Delpuech JJ, Martin GJ: Practical NMR Spectroscopy. Philadelphia, Heyden and Son, 1980

39. Litt L, Espanol MT, Xu Y, Cohen Y, Chang L-H, Weinstein PR, Chan PH, James TL: *Ex vivo* multinuclear NMR spectroscopy of perfused, respiring rat brain slices: Model studies of hypoxia, ischemia, and excitotoxicity, Biological NMR Spectroscopy. Edited by Markley JL, Opella SJ. New York, Oxford University Press, 1997

40. Remy C, Albrand JP, Benabid AL, Decorps M, Jacrot M, Riondel J, Foray MF: *In vivo* ^{31}P nuclear magnetic resonance studies of T_1 and T_2 relaxation times in rat brain and in rat brain tumors implanted to nude mice. Magn Reson Med 1987; 4:144–52

41. Kauppinen RA, Williams SR: Cerebral energy metabolism and intracellular pH during severe hypoxia and recovery: A study using ^{1}H, ^{31}P and $^{1}H[^{13}C]$ nuclear magnetic resonance spectroscopy in the guinea pig cerebral cortex *in vitro*. J Neurosci Res 1990; 26:356–69

42. Petroff OA, Prichard JW, Behar KL, Alger JR, den Hollander JA, Shulman RG: Cerebral intracellular pH by ^{31}P nuclear magnetic resonance spectroscopy. Neurology 1985; 35:781–8

43. Cohen MM, Pettegrew JW, Kopp SJ, Minshew N, Glonek T: P-31 nuclear magnetic resonance analysis of brain: Normoxic and anoxic brain slices. Neurochem Res 1984; 9:785–801